J. Parallel Distrib. Comput. 74 (2014) 2831–2844

Contents lists available at ScienceDirect

J. Parallel Distrib. Comput.

journal homepage: www.elsevier.com/locate/jpdc

Accident aware localization mechanism for wireless sensor networks

Chao-Tsun Chang [a], Chih-Yung Chang [b,*], Tzu-Lin Wang [b]

[a] Hsiuping University of Science & Technology, Taichung, Taiwan
[b] Tamkang University, Taiwan

HIGHLIGHTS

- Improving the location accuracy with off-the-shelf hardware.
- Active location detection and correction with low computing complexity for each sensor.
- The proposed ALCP mechanism is energy efficient for location-error detection and correction.
- Complete analysis and extensive simulations to verify the performance of the ALCP.

ARTICLE INFO

Article history:
Received 11 April 2013
Received in revised form
31 March 2014
Accepted 20 May 2014
Available online 2 June 2014

Keywords:
Location correction
Bounding box
Localization
Wireless sensor networks

ABSTRACT

Accurate location information is important for event reporting, coverage estimation, and location-aware routing in a Wireless Sensor Network (WSN). Recently, a number of range-free localization schemes have been proposed to provide each static sensor with location information, which is represented by a rectangular region. However, most WSN applications are applied in outdoor environments where the sensors' location regions could be incorrect due to sudden accidents. This paper proposes an Active Location Correction Protocol, called ALCP, for detecting and correcting the occurrence of location error based on the bounding box technology. Performance study reveals that applying the ALCP to improve the location accuracies can enhance the performance of the well-known GPSR routing in terms of routing length, sensing coverage, and packet arrival rate.

1. Introduction

In a WSN, locations of sensor nodes are critical information in most applications of WSN, such as coverage calculation, event detection, object tracking, and location-aware routing. The sensor nodes have to be aware of their locations to specify "where" a certain event occurs. The simplest way for obtaining the location information is to equip each sensor node with a *Global Positioning System* (*GPS*). However, it leads to expensive hardware cost and considerable power consumption. To reduce hardware cost, a number of location discovery schemes have been proposed in recent years. These schemes [10,17] share the common feature wherein some static beacon nodes (or anchors), which are aware of their own location information, are deployed in the WSN. All the other sensor nodes discover their locations based on the information provided by these beacon nodes. These schemes still have the undetermined location accuracy of each sensor node since they highly depend on the number and deployed positions of the static anchors. To obtain high location accuracy, the number of anchor nodes tends to be increased, which adds to the localization cost. Another problem is that the static anchors play no role after broadcasting the beacons [8].

Studies [4,5,23,19,22,8,26,20,15,16,21,18,6] proposed a mobile anchor localization mechanism for a resource-constrained WSN. Each mobile anchor is aware of its own location information by equipping the GPS or other location support system. In previous works [8,26,20,15,13], the mobile anchor broadcasts its coordinates at certain locations which can be treated as the virtual static anchor at those locations. Upon receiving the coordinate packet, each static sensor can locally identify whether it is located within the communication range of the mobile anchor. When a static sensor receives multiple coordinate packets from the mobile anchor, the static sensor can calculate its new estimative region by the intersection of all possible location regions. To simplify the calculation of estimative region, studies [8,26,20,18] treat the communication circle of each sensor as the quadratic region, called *bounding box*.

* Corresponding author.
E-mail addresses: cctas@mail.hust.edu.tw (C.-T. Chang), cychang@mail.tku.edu.tw, cychang@cs.tku.edu.tw (C.-Y. Chang), tlwang@wireless.cs.tku.edu.tw (T.-L. Wang).

http://dx.doi.org/10.1016/j.jpdc.2014.05.006
0743-7315/

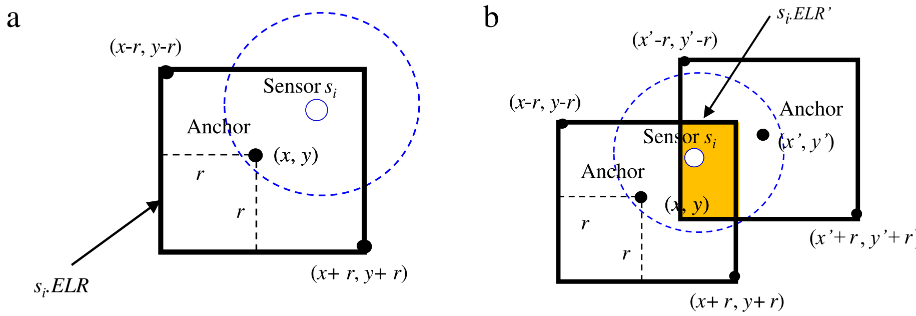

Fig. 1. (a) If sensor s_i receives the location (x, y) from the mobile anchor, and its communication range is r, the *Estimated Location Region* can be represented by $(x-r, y-r)-(x+r, y+r)$ or $s_i.ELR$. (b) The area of $s_i.ELR'$ can be determined by the $s_i.ELR$ and the anchor's broadcast message. (For interpretation of the references to color in this figure legend, the reader is referred to the web version of this article.)

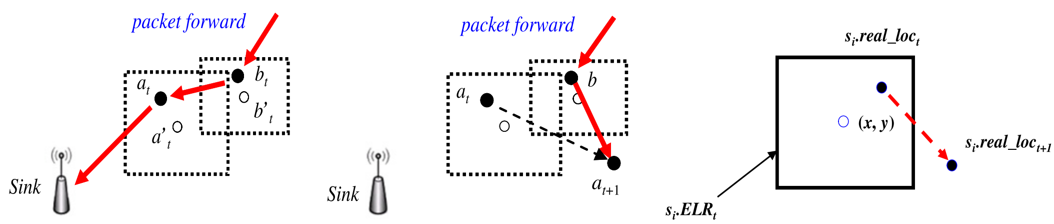

(a) In location-aware routing, the packets from sensor b to the sink can be forwarded by sensor a at time t. The circle a'_t and dot a_t denote the center of the *ELR* and the actual location of the sensor a, respectively.

(b) When sensor a is moved at time $t+1$ in the accident, the location error might lead to a situation that sensor a forwards the data packet to a location which is far away from the sink.

(c) Sensor s_i has a location error at time $t+1$ if $s_i.real\_loc_{t+1} \notin s_i.ELR_t$.

Fig. 2. An example illustrating the location error and impact on the location-aware routing.

The mobile anchor mainly helps the static sensors to estimate their locations by periodically broadcasting its location. Let the location and communication range of a mobile anchor be (x, y) and r, respectively. The bounding box of the sensor s_i can be presented by $(x-r, y-r)-(x+r, y+r)$ and denoted by an *Estimated Location Region* (or $s_i.ELR$), as shown in Fig. 1(a). In Fig. 1(a), sensor s_i determines that it is located in $s_i.ELR$ when it receives the location message (x, y) from the mobile anchor. As shown in Fig. 1(b), upon receiving the location messages (x, y) and (x', y') which are sent by the mobile anchor, sensor s_i intersects two *ELR* regions to determine its new region $s_i.ELR'$ which is presented by $(x'-r, y-r)-(x+r, y'+r)$, marked by yellow ink. Consequently, this observation indicates that the original localization accuracy of sensor s_i, represented by the area size of $s_i.ELR$, can be improved by receiving a new broadcasting rectangle from the anchor.

Since most WSN applications are applied in an outdoor environment, the real location of each static sensor could be changed due to unexpected events, such as malicious changes, hurricanes, and mudflows. For example, detecting intruders crossing an international border is increasingly being seen as an important application for wireless sensor networks [14,25]. The barrier construction using the static sensors has been considered to reduce the patrolling cost. Take the border between America and Mexico as an example. The length of the border is about 3000 km. This border crosses two wide deserts, Sonoran and Chihuahuan, which frequently have strong breezes. In this scenario, the sensors should maintain high localization accuracy for reporting the accurate location of an intruder. However, the strength of the strong breeze in the deserts can be higher than 17 m/s, which can easily cause sensors to move, resulting in location errors for sensor nodes. The deserts of China are another example. The deserts in the Junggar Basin have strong breeze with strength of 17 m/s for an average of 80 days in a year [11]. The location errors will impact the effectiveness of the monitoring tasks, such as the coverage, target tracking, and packet routing.

The accidents could raise a location error problem where the real location of the sensor is out of its *ELR*. Fig. 2(a) and (b) show an example to illustrate the impact of location error on routing. In Fig. 2(a), the packet sent from sensor b to the sink node can be forwarded by sensor a at time t by applying the location-aware routing. When sensor a is moved at time $t+1$ due to the accident, the location error leads to a situation where sensor a forwards the packet to a location which is far away from the sink, as shown in Fig. 2(b). Let the real location of sensor s_i at time t be $s_i.real\_loc_t$. If $s_i.real\_loc_{t+1}$ is moved due to an accident such that the condition $s_i.real\_loc_{t+1} \notin s_i.ELR$ is satisfied, sensor s_i has a *location error* at time $t+1$, as shown in Fig. 2(c). The location error will further degrade the performance of coverage estimation, tracking, or packet routing.

This paper aims to develop an active location correction protocol based on the bounding box technique. The proposed *ALCP* mechanism actively detects the location errors and cooperates with the neighboring sensors to correct the *ELR* information. The remaining part of this paper is organized as follows. Section 2 gives the related works of localization and location error detection mechanisms while Section 3 illustrates the network environment and problem formulation of the proposed scheme. Section 4 details the proposed active location correction mechanism and presents the analysis of its impact on routing. Section 5 compares the proposed mechanisms with existing works. Section 6 presents the conclusion.

2. Related work

Localization with low cost and high accuracy is very important in wireless sensor networks [26,20,15,7,24]. To eliminate the requirement of deploying a large number of static anchors in WSN, studies [8,26,20,15,16,21,18,6] have been proposed for a resource-constrained WSN. In studies [26,20,15,16,21,18], a mobile anchor that is aware of its own location is proposed to periodically move and broadcast a beacon which contains its coordinates in order to improve the location accuracy of nearby static sensors. Upon receiving the beacon message, the sensor node knows that it is within the region of the circle centered at the coordinates with a radius of r, where r is the communication range. Therefore, the sensor node identifies that its location is within the *estimative circle region*. Based on the range-constraints of beacon messages, the static sensor receives several coordinates from the mobile anchor and its estimative circle region may be reduced by calculating the intersected regions of its neighbors and itself. However, the range-constraint localization highly depends on the location information of one-hop neighbors of the mobile anchor. Once the one-hop neighbors of mobile anchor have location errors, the location accuracy will be decreased.

Srinath T.V. [21] extends the range-constraint from one-hop to two-hop neighboring sensors. Let $A = \{a_1, a_2, \ldots, a_n\}$ denote n neighbors of the mobile anchor and B_i denote those sensors that are neighbors to sensor a_i in set A. Upon receiving the location information from the mobile anchor, all sensors in set A calculate and then broadcast their estimative region information. Since the two-hop sensors of mobile anchor cannot receive the location information from the mobile anchor, nodes in set B_i have a location constraint which are not located in the estimative region of a_i. In addition, the nodes in set B_i neighbors to node a_i imply that they are located in the communication range of any possible location of a_i. Based on the above-mentioned two constraints, nodes in set B_i can also derive their own estimative regions. Although different coordinates received from the mobile anchor can help reduce the size of static sensor's estimative region, improving the location accuracy, it is complex and time consuming to calculate the intersection region of several circle regions. Consequently, studies [20,18] proposed localization schemes which apply a rectangle region, called *Estimated Location Region* (*ELR*), instead of a circle region to simplify both the calculation and representation of the new estimative region.

Since most WSN applications are applied in outdoor environments, the actual location of each static sensor might be changed due to unexpected events. The accidents could raise a location error problem where the actual location of the sensor is out of its *ELR*. In recent years, a number of studies proposed the schemes for location verification [15,3,7,24,1]. The TDoA method proposed in [3] verifies the estimated location of nodes by using the sum of propagation time and received RF signal strength to measure the distance between any two nodes. A previous study [1] estimated the signal strength of neighboring nodes for determining whether or not the monitoring nodes are moved. Although the schemes considering the signal strength and location error threshold are able to evaluate the location error, the distance measurement with signal strength needs some special hardware. Another study [7] applied the strategy of consistency check to verify whether or not the current locations of nodes are consistent with the group-based deployment model and the deployment knowledge. In [24], the centralized verification schemes, called *Greedy Filtering by Matrix* (*GFM*) and *Trustability Indicator* (*TI*), are proposed to detect abnormal location by using the information of neighboring nodes. In [15], a beacon movement detection scheme was proposed; it applies simple beacons and location error threshold to decide whether or not a sensor's neighbor is moved. In [1], a movement diction mechanism verifies the neighboring node movement by using the information of local neighbors and mobility metrics, including the occurrence of isolation periods, the number of long-term neighbors, the fraction of total neighbors, the neighbor longevity index, and the neighborhood changes. However, most of them cannot reduce the impact of a location error existing in WSN before re-localization. To our knowledge, previous works failed to address the issue of how to detect a location error and correct it by a guaranteed measurement for the WSN. To address this problem, this paper proposes an active location correction protocol for detecting and correcting a location error. The proposed *ALCP* scheme helps each sensor to identify its actual *ELR*, maximize its location accuracy, and hence improve the routing performance.

3. Network environment and foundations

This section introduces the considered network environment and location error problem. The impact of location error on the location-aware routing is presented.

3.1. Network environment

The considered WSN $N = \{s', s_1, s_2, \ldots, s_n\}$ consists of a sink s' and n static sensor nodes. Sensor nodes are uniformly deployed in a monitoring area. Recall that the notation $s_i.real\_loc_t$ denotes the location of sensor node s_i at time t. By applying the localization mechanisms [20,15], each sensor s_i is aware of its location information, which is a rectangular region represented by $s_i.ELR$, where $s_i.real\_loc_t \in s_i.ELR$.

3.2. Problem statements

A sensor s_i is said to be location error at time t if it moved by accident at time t such that condition $s_i.real\_loc_t \notin s_i.ELR$ is satisfied. Since the sensor cannot be aware of its movement, the location information *ELR* of that sensor, as maintained in the memory, is not changed even if its actual location is out of its maintained region *ELR*. Fig. 2(c) shows that sensor s_i has a location error. Given a set of moved sensors $N' \subseteq N$, the *Movement-driven Location-error Problem* [15] asks the sensors $s_i \in N'$ to detect the location errors and to relocate their locations such that $s_i.real\_loc_t \in s_i.ELR$ is satisfied at any given time t. Recall that notation r denotes the communication range of sensor s_i and $|s_i.ELR|$ denotes the area size of $s_i.ELR$. In the proposed *ALCP*, the localization accuracy of sensor s_i, denoted by $A(s_i)$, can be measured by the value of $|s_i.ELR|$ when $s_i.real\_loc \in s_i.ELR$ is satisfied. A smaller value of $|s_i.ELR|$ indicates that sensor s_i has higher localization accuracy. On the other hand, the value of $A(s_i)$ will be set to zero when sensor s_i has a location error. Let $A(N)$ denote the average localization accuracy of all sensors in network N, as shown in Eq. (1). The proposed *ALCP* scheme aims at detecting and correcting the location errors of the sensors and hence achieves the goal of this paper.

$$\text{Maximize } A(N), \quad \text{where } A(N) = \frac{1}{n}\sum_{i=1}^{n} A(s_i),\ s_i \in N. \tag{1}$$

The maximal network accuracy will improve the performance of location-aware routing, which is highly impacted by the location error.

3.3. Impact of location error

The location error will create overheads to the location-aware routing, and hence reduce the network performance. Fig. 3(a) and (b) show the impact of location error on the location-aware routing. Fig. 3(a) and (b) assume that the sensors s_1 and s_{11} are source and destination nodes of a given route, respectively. By applying the well-known location-aware routing protocol GPSR [12], the routing path s_1–s_2–s_7–s_9–s_{11} is constructed, as shown in Fig. 3(a). In a situation where sensor s_7 is moved to a new location, the location error problem occurs, as shown in Fig. 3(b).

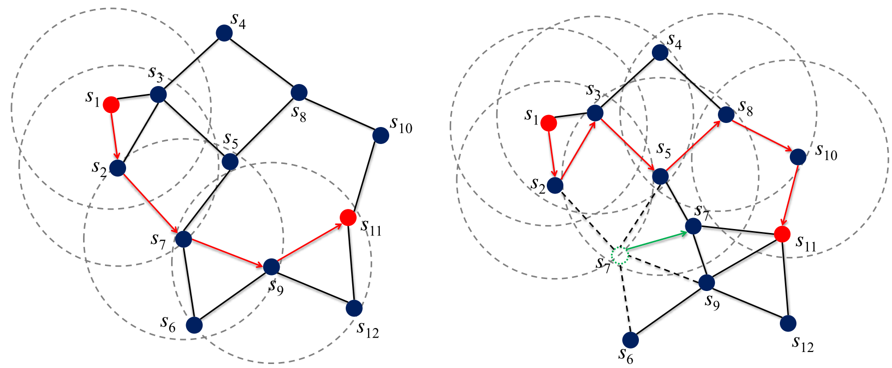

(a) The routing path construction before the location error.

(b) The routing path change due to the location error.

Fig. 3. An example illustrating the impact of the location-aware routing caused by location errors. The red arrows denote the routing path of the packets.

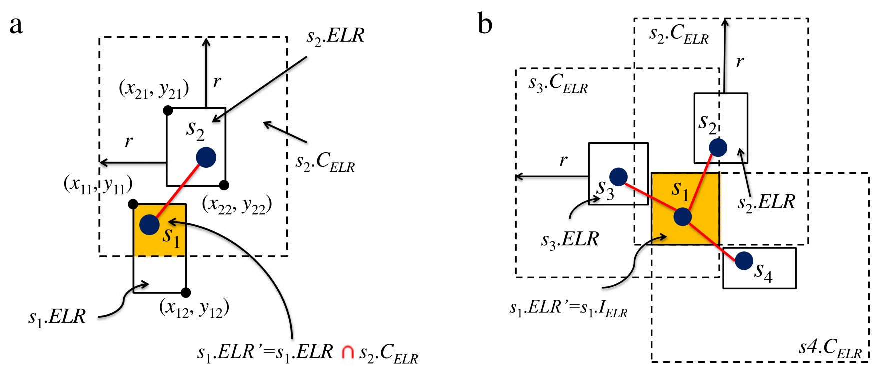

Fig. 4. (a) The area size of $s_1.ELR$ can be reduced by $s_2.C_{ELR}$. (b) The area of $s_1.ELR'$ can be determined by the $s_1.I_{ELR}$.

In Fig. 3(b), when the location error of sensor s_7 occurs, sensor s_2 cannot send the packet to s_7 and thus sensor s_2 changes the routing path from s_2–s_7–s_9–s_{11} to s_2–s_3–s_5–s_8–s_{10}–s_{11}. The major reason for this is that sensor s_2 cannot successfully send its data to sensor s_7. Therefore, sensor s_2 forwards its data to its neighbor s_3. According to GPSR routing protocol, the packet will be sent from s_3 to s_5. Since sensor s_5 is not aware of the new neighboring node s_7, it forwards the packet to s_8. Then the packet is subsequently forwarded from s_8 to s_{11} along the route s_8–s_{10}–s_{11}. In fact, sensor s_5 can directly send the packets to sensor s_7 if s_5 and s_7 can detect and correct the location error of sensor s_7 in time. The routing overhead increases about 20% in this case due to the location error. This paper aims to propose a distributed scheme for detecting and correcting the location errors by using the *ELR* information. By applying the proposed *ALCP* scheme, location error of the sensors can be efficiently detected and corrected. The impact of location error on applications that highly depend on the location information such as coverage and routing can be eliminated.

4. The active location correction protocol

This section presents the proposed *ALCP* for location error problems in WSN. First, the notations of the proposed scheme are defined. Then, the basic concepts and examples related to the proposed scheme are introduced, and the algorithms of the proposed *ALCP* are detailed. Finally, the analysis of location impact on routing is presented.

4.1. Notations of ALCP

The proposed *ALCP* is based on the bounding box technique. Some terms used in describing the proposed *ALCP* are defined.

Definition (*Communication Range of ELR* (C_{ELR})). Let $s_i.C_{ELR}$ denote the maximum area where any sensor outside this area cannot communicate with sensor s_i. Let $s_i.ELR$ be the area of $(x_1, y_1) - (x_2, y_2)$. The area of $s_i.C_{ELR}$ is defined by $(x_1-r, y_1-r)-(x_2+r, y_2+r)$, where r denotes the communication range of any sensor. □

Definition (*Intersection of Neighbor's* C_{ELR} (I_{ELR})). Let $N_t(s_i)$ represent the neighboring sensors of sensor s_i at time t. The intersection of neighbor's *ELR*, denoted by I_{ELR}, of sensor s_i at time t is defined as

$$s_i.I_{ELR_t} = \bigcap_{s_j \in N_t(s_i)} s_j.C_{ELR}. \quad \square$$

Notice that $s_i.I_{ELR}$ indicates another *ELR* information of sensor s_i, which can be determined by the intersection of its neighbors' C_{ELR}. When sensor s_i has a location error, the information of $s_i.ELR$ will be replaced to $s_i.I_{ELR}$ in the location correction process.

Fig. 4(a) and (b) show the examples of C_{ELR} and I_{ELR} applied in the proposed *ALCP*. The red line depicts the neighboring relationship between sensors while the notation $s_1.ELR'$ denotes the new estimated *ELR* of sensor s_1. Fig. 4(a) shows that the area size of $s_1.ELR$ can be reduced by $s_2.C_{ELR}$, where sensors s_1 and s_2 are neighbors. Since sensor s_1 locates at region $s_2.C_{ELR}$, the new region $s_1.ELR'$ can be determined by computing $s_1.ELR \cap s_2.C_{ELR}$ and the area of $s_1.ELR'$ will be $(x_{11}, y_{11})-(x_{12}, y_{22}+r)$, as shown in Fig. 4(a). This computation is especially useful to reduce the area size of $s_1.ELR$. Furthermore, the I_{ELR} can be applied to evaluate the new *ELR* of a sensor when it has a location error in WSN. As shown in Fig. 4(b), when sensor s_1 has location error and its *ELR* becomes unreliable, it can compute its new location region $s_1.ELR'$ according to the C_{ELR} of its neighbor nodes s_2, s_3, and s_4. Recall that C_{ELR} represents the maximum area where any sensor outside this area cannot communicate with the sensor. The region $s_1.ELR'$ can be obtained by computing the following expression:

$$s_1.ELR' = s_1.I_{ELR} = s_2.C_{ELR} \cap s_3.C_{ELR} \cap s_4.C_{ELR}.$$

The details of the proposed *ALCP* will be described in the next section.

4.2. Basic concepts of ALCP

To present in detail the proposed *ALCP* for detecting and correcting the location error in WSN *N*, some important properties of the *ELR* are introduced as follows.

Lemma 1. *If sensor s_a can communicate with sensor s_b and both of their ELRs are correctly estimated, the following properties hold.* (1) $s_a.ELR \subseteq s_b.C_{ELR}$ *and* (2) $s_b.ELR \subseteq s_a.C_{ELR}$.

Proof. (1) Assume $s_a.ELR \nsubseteq s_b.C_{ELR}$. According to the definition of C_{ELR}, it implies that $s_a.real\_loc \notin s_b.C_{ELR}$ and sensor s_a cannot communicate with sensor s_b. This inference contradicts with the given hypothesis. (2) The proof is similar to (1). □

Herein, we notice that a sensor does not need to correct its *ELR* if its real location is within its *ELR* even if it is moved due to an accident. That is, the movement of sensor s_i is tolerable and hence the computation of $s_i.ELR_{t+1}$ is not needed at time $t+1$ if condition $s_i.real\_loc_{t+1} \in s_i.ELR_t$ is satisfied, even if $s_i.real\_loc_{t+1} \neq s_i.real\_loc_t$. Since the moved sensor s_i cannot be aware of its movement and considering that $s_i.real\_loc_t \in s_i.ELR_t$, the movement detection relies on the location information reported from its neighbors. In what follows, some properties are introduced to establish the fundamentals of the proposed scheme.

Theorem 1. *If $s_i.real\_loc_t \in s_i.ELR_t$, $s_i.real\_loc_t \in s_i.I_{ELR_t}$.*

Proof. Let sensor s_a be any neighbor of sensor s_i. Since sensors s_a and s_i can communicate with each other, $s_i.real\_loc_t \in s_i.ELR_t \subseteq s_a.C_{ELR_t}$ (according to Lemma 1). This implies that $s_i.real\_loc_t \in s_i.I_{ELR_t}$. □

If $s_i.real\_loc_t \notin s_i.I_{ELR_{t+1}}$, this means that there exists at least one neighbor of sensor s_i, say s_a, such that $s_i.real\_loc_t \notin s_a.C_{ELR_{t+1}}$. As a result, $s_i.real\_loc_t$ is not included in $s_a.C_{ELR_{t+1}}$ and hence $s_i.real\_loc_{t+1} \notin s_i.ELR_t$. Theorem 2 reflects this argument.

Theorem 2. *If $s_i.ELR_t$ cannot be included in $s_i.I_{ELR_{t+1}}$, sensor s_i has moved out of the region of $s_i.ELR_t$.* □

Herein, assume that each sensor s_i can exchange its device ID and $s_i.ELR_t$ information with its neighbors when it detects the changes of its neighbors. The following terms are defined for presenting the proposed *ALCP*. Sensor s_i satisfies the condition $s_i.real\_loc_t \in s_i.I_{ELR_{t+1}}$, which is called *reliable* node. If sensor s_i is reliable originally but satisfies the condition $s_i.ELR_t \nsubseteq s_i.I_{ELR_{t+1}}$, it will become *unreliable* at time $t+1$. This indicates that the neighboring sensors can help the unreliable sensor to detect that itself as unreliable.

Fig. 5 gives an example of WSN localized by applying the bounding box localization mechanism [26,20]. When the localization is completed, all sensor nodes are reliable and have their own *ELR*. Let ELR_{org} denote the *ELR* of the sensor before initiating *ALCP*. However, the *ELR* of some sensors could be incorrect due to accidents. As shown in Fig. 6, assume that the sensor s_7 is moved to a new location. Sensors s_2 and s_6 are aware that the neighbor s_7 has disappeared and sensor s_{11} will find a new unreliable neighbor s_7 at the same time. But sensors s_5 and s_9 do not detect the change of s_7 since they still can communicate with s_7 and measure that $s_7.ELR_t \subseteq s_5.C_{ELR_t}$ and $s_7.ELR_t \subseteq s_5.C_{ELR_t}$. Consequently, sensors

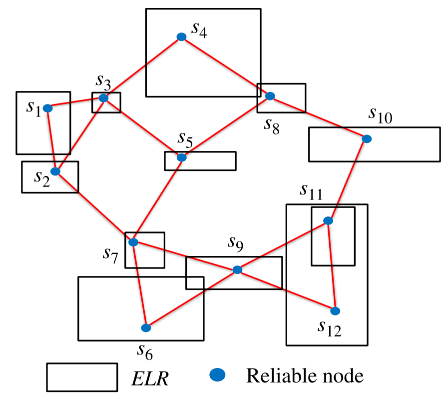

Fig. 5. An example of WSN to depict the reliable node and reliable neighboring.

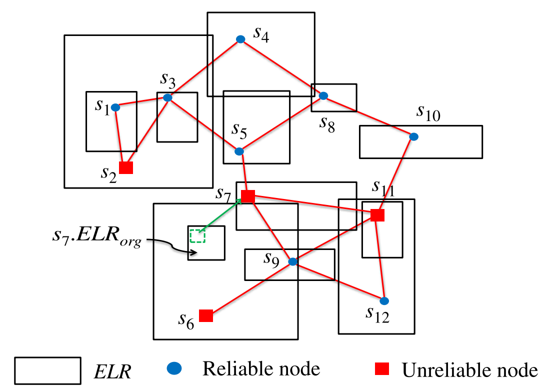

Fig. 6. The location of sensor s_7 presented in Fig. 5 is changed due to an accident so that its estimated location region will become location error.

s_2, s_6, s_7, and s_{11} detect the variations of their neighbors. If the location error cannot be corrected, the overhead of the location-aware routing will be increased, resulting in low network performance.

Let $C_u(s_i)$ denote the degree of unreliability of sensor s_i which indicates the number of changed neighbors of sensor s_i. A sensor, say s_i, with a high value of $C_u(s_i)$ means that it becomes unreliable with large changes in the neighboring relationship. The following rules will be applied to evaluate the value of $C_u(s_i)$ of each sensor s_i for detecting the location error.

Rule 1. If $s_i.real\_loc \in s_i.ELR$, set $C_u(s_i) = 0$.

Rule 2. If $s_i.ELR_t \nsubseteq s_i.I_{ELR_{t+1}}$, set $C_u(s_i) = C_u(s_i) + 1$.

Rule 3. If ($s_j \notin N_t(s_i)$ and $s_j \in N_{t+1}(s_i)$) or ($s_j \in N_t(s_i)$ and $s_j \notin N_{t+1}(s_i)$), set $C_u(s_i) = C_u(s_i) + 1$.

Rule 1 applies the initial value for $C_u(s_i)$. Rule 2 handles the change influences arising from the neighbors' absences, while Rule 3 handles the change influences caused by the introduction of new neighbors.

In the literature, a number of localization mechanisms based on bounding box technology [20,6] have been proposed to provide the basic location information of sensor nodes. The proposed *ALCP* mainly consists of two phases: *Detection and Primary Correction* (*DPC*) and *Refined Correction* (*RC*) phases. Let ELR_{dpc} and ELR_{rc} denote the *ELR* obtained in the *DPC* and *RC* phases, respectively. The *DPC* phase is designed for detecting the location error and determining ELR_{dpc} for the damage node according to the ELR_{org} of each neighboring reliable node. Then, the *RC* phase refines the correction to calculate ELR_{rc} for the damage node. The detailed processes of the *DPC* and *RC* phases are introduced as follows.

In the *DPC* phase, each sensor s_i firstly calculates the value of $C_u(s_i)$. If the value $C_u(s_i)$ is not zero, it becomes an unreliable node. Otherwise, it terminates the process of the *DPC* phase. Assume that sensor s_i is an unreliable node. Initially, it will determine its $s_i.ELR_{dpc}$ according to the *ELR* measurements of its neighbors, including those reliable and unreliable neighbors which have smaller degree of unreliability than itself. Let $s_i.C_{ELR}^{org}$ and $s_i.C_{ELR}^{dpc}$ denote the maximum area where any sensor outside the area $s_i.ELR_{org}$ and $s_i.ELR_{dpc}$ cannot communicate with sensor s_i. The value of I_{ELR} of sensor s_i can be evaluated by

$$s_i.I_{ELR} = (\cap s_j.C_{ELR}^{org}) \cap (\cap s_k.C_{ELR}^{dpc}) \tag{2}$$

where $C_u(s_j) = 0$, for all $s_j \in N_t(s_i)$, and $C_u(s_k) < C_u(s_i)$, for all $s_k \in N_t(s_i)$. If the area $s_i.ELR_{org}$ is included in the new measurement $s_i.I_{ELR}$, the area $s_i.ELR_{dpc}$ will be set by $s_i.ELR_{org}$. Otherwise, the value of $s_i.ELR_{dpc}$ will be set by $s_i.I_{ELR}$. When sensor s_i determines $s_i.ELR_{dpc}$, it will send the information of $s_i.ELR_{dpc}$ to help its unreliable neighbors which have larger degree of unreliability than itself. Once ELR_{dpc} is measured, the *DPC* phase is completed and then the *RC* process will be applied. Let n_b be the average number of the neighboring nodes of the sensors. The time complexities of the *DPC* algorithm is $O(n_b)$ since the *DPC* algorithm calculates the ELR_{dpc} according to the ELR_{org} of their neighboring nodes.

The major task of the *RC* phase is that sensor s_i will wait and receive the ELR_{rc} from its unreliable neighbors with larger degree of unreliability than itself to refine its *ELR* measurement and determine the $s_i.ELR_{rc}$. This is not straightforward since the sensors with larger unreliability degree will be used to improve the neighboring sensors with smaller unreliability degree. The following illustrates that operations designed in the *RC* phase can further improve the location accuracy of some sensors. The I_{ELR} measurement of sensor s_i can be evaluated by

$$s_i.I_{ELR} = s_i.ELR_{dpc} \cap (\cap s_j.C_{ELR}^{dpc}), \tag{3}$$

where $C_u(s_i) < C_u(s_j)$, for all $s_j \in N_t(s_i)$.

***DPC Algorithm*: Detection and Primary Correction (*DPC*) Phase**

// This algorithm is executed by each sensor s_i.
// Assume that sensor s_i and its *ELR* is $s_i.ELR_{org}$.
// Let T_{days} denote the number of days that the *DPC* algorithm of *ALCP* should be triggered for executing error detection and correction of sensor location.
// By Rule 1, set $C_u(s_i) = 0$ when localization is finished.

1. Repeat the following operations every T_{days} // Trigger *DPC* algorithm
2. { for all s_i
 {listen and send the beacons to $s_j \in N_t(s_i)$;}
3. Execute Rules 2, 3, and compute the value of $C_u(s_i)$;
4. if $C_u(s_i) = 0$, return;
5. for all s_j, where $C_u(s_j) = 0$ and $s_j \in N_t(s_i)$
6. $s_i.I_{ELR} = \cap s_j.C_{ELR}^{org}$; // $s_j.C_{ELR}^{org}$ is obtained from $s_j.ELR_{org}$
7. if $\{s_j \mid s_j \in N_t(s_i)$ and $C_u(s_i) > C_u(s_j)\}$ is not empty, {
8. wait and receive the information of $s_j.ELR_{dpc}$, where $s_j \in N_t(s_i)$ and $C_u(s_i) > C_u(s_j)$;
9. for all s_k, where $s_k \in N_t(s_i)$ and $C_u(s_i) > C_u(s_k)$
10. $s_i.I_{ELR} = s_i.I_{ELR} \cap s_k.C_{ELR}^{dpc}$; // $s_k.C_{ELR}^{dpc}$ is obtained by $s_k.ELR_{dpc}$
11. }
12. if $(s_i.ELR_{org} \subseteq s_i.I_{ELR})$
13. $s_i.ELR_{dpc} = s_i.ELR_{org}$;
14. else $s_i.ELR_{dpc} = s_i.I_{ELR}$;
15. send the information of $s_i.ELR_{dpc}$ to node s_j, where $s_j \in N_t(s_i)$ and $C_u(s_j) < C_u(s_i)$;
16. execute the *RC* algorithm. }

In Fig. 7(a), $s_a.ELR_{dpc}$, $s_b.ELR_{dpc}$, and $s_c.ELR_{dpc}$ are determined in the *DPC* phase, where $C_u(s_a)$, $C_u(s_b)$, and $C_u(s_c)$ are 1, 2, and 1, respectively. In the *DPC* phase, sensor b applies Eq. (2) to determine $s_b.ELR_{dpc}$ by calculating the intersection of $s_b.I_{ELR}$, $s_a.C_{ELR}$, and $s_c.C_{ELR}$, where $s_a.C_{ELR}$ and $s_c.C_{ELR}$ are calculated by $s_a.ELR_{dpc}$ and $s_c.ELR_{dpc}$. Fig. 7(b) shows that sensor s_b in the *RC* phase will send the information of $s_b.ELR_{rc}$ to its neighbors a and c. Upon receiving the information of $s_b.ELR_{rc}$, sensors a and b are able to reduce the area size of $s_a.ELR_{dpc}$ or $s_c.ELR_{dpc}$. In Fig. 7(b), since the value of $|s_b.I_{ELR}|$ evaluated in Eq. (3) might be smaller than the value of $|s_b.ELR_{dpc}|$, the value of $|s_b.ELR_{rc}|$ can be smaller than the value of $|s_a.ELR_{dpc}|$ or $|s_c.ELR_{dpc}|$. Therefore, if sensor s_c updates its *ELR* based on the information of $s_b.ELR_{rc}$, it might have a smaller value of $|s_c.ELR_{rc}|$ than $|s_c.ELR_{dpc}|$ even though $C_u(s_c) < C_u(s_b)$.

***RC Algorithm*: Refined Correction (*RC*) Phase**

// Sensor s_i with $C_u(s_i) \neq 0$ executes the algorithm.
// $s_i.ELR_{dpc}$ denotes the *ELR* estimated in *DPC* phase.
// $s_i.ELR_{rc}$ denotes the *ELR* estimated in *RC* phase.

1. $s_i.I_{ELR} = s_i.ELR_{dpc}$;
2. if $\{s_j \mid s_j \in N_t(s_i)$ and $C_u(s_i) < C_u(s_j)\}$ is not empty {
3. wait and receive the information of $s_j.ELR_{rc}$, where $s_j \in N_t(s_i)$ and $C_u(s_i) < C_u(s_j)$;
4. for all s_j, where $s_j \in N_t(s_i)$ and $C_u(s_i) < C_u(s_j)$
 // $s_j.C_{ELR}$ is obtained by $s_j.ELR_{rc}$.
5. $s_i.I_{ELR} = s_i.I_{ELR} \cap s_j.C_{ELR}$;
6. }
7. if $(|s_i.I_{ELR}| < |s_i.ELR_{dpc}|)$
8. $s_i.ELR_{rc} = s_i.I_{ELR}$;
9. else
10. $s_i.ELR_{rc} = s_i.ELR_{dpc}$;
11. send the information of $s_i.ELR_{rc}$ to node s_j, where $s_j \in N_t(s_i)$ and $C_u(s_i) > C_u(s_j)$;
12. $C_u(s_i) = 0$; // node s_i reset to reliable.

The detailed operations designed in the *RC* phase are presented below. Initially, sensor s_i sets $s_i.ELR_{rc}$ by $s_i.ELR_{dpc}$ if there exists no neighbor s_j with $C_u(s_i) < C_u(s_j)$. Otherwise, sensor s_i will wait and receive the information of $s_j.ELR_{rc}$ from s_j, where $s_j \in N_t(s_i)$ and $C_u(s_i) < C_u(s_j)$. Herein, sensor s_i intends to improve its I_{ELR} measurement by calculating $s_i.I_{ELR} = s_i.ELR_{dpc} \cap s_j.C_{ELR}$, where $s_j.C_{ELR}$ is measured by its unreliable neighbors' $s_j.ELR_{rc}$. If the area size of $s_i.I_{ELR}$ is smaller than that of $s_i.ELR_{dpc}$, $s_i.ELR_{rc}$ will be set to $s_i.I_{ELR}$. Otherwise, $s_i.ELR_{rc}$ will be set to $s_i.ELR_{dpc}$. When sensor s_i determines $s_i.ELR_{rc}$, it will send the information of $s_i.ELR_{rc}$ to help its unreliable neighbor s_j for computing the $s_j.ELR_{rc}$, where $s_j \in N_t(s_i)$ and $C_u(s_i) > C_u(s_j)$ and then the *RC* phase is completed. Let n_b be the average number of the neighboring nodes of the sensors. The time complexities of the *RC* algorithm is $O(n_b)$ since the *RC* algorithm calculates the ELR_{rc} according to the ELR_{dpc} of their neighboring nodes.

In *ALCP*, each sensor informs its existence to the neighboring nodes by the beacons and receives the messages from their neighbors. Within a given time, each sensor calculates its value of $C_u()$ by the received messages. After that, each sensor exchanges the value of $C_u()$ with their neighbors and then initiates the location error detection in the *DPC* phase. If the location error occurs, the *RC* phase will be executed. The frequency of the beacons and the communication cost highly depend on the location accuracy requirements of the concerned applications. Let n_b be the average number of the neighboring nodes of each sensor. The communication cost of the *DPC* and *RC* algorithms are all $O(n_b)$, which is similar to the time complexity. The *DPC* and *RC* algorithms present the detailed processes of the *Detection and Primary Correction* and *Refined Correction* phases, respectively.

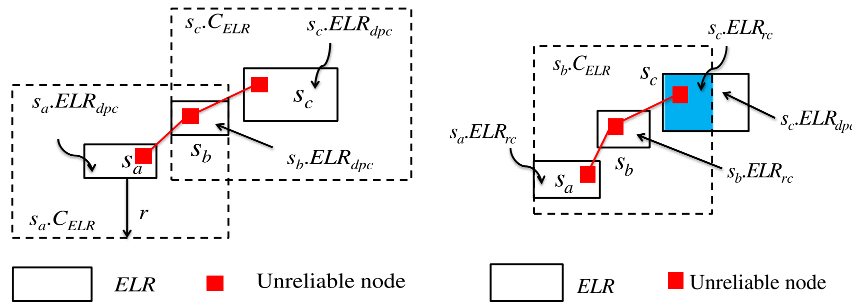

(a) The sensors' ELR_{dpc} is determined in the *DPC* phase.

(b) The sensors' ELR_{rc} is determined in the *RC* phase.

Fig. 7. An example for illustrating the ELR_{dpc} measurement which can be improved in *RC* phase.

Consider the example depicted in Fig. 6. Since the values of $C_u(s_2)$, $C_u(s_6)$, $C_u(s_7)$, and $C_u(s_{11})$ are 1, 1, 3, and 1, respectively, sensors s_2, s_6, s_7, and s_{11} will initiate the *DPC* phase of the proposed *ALCP*. In the example, the unreliable sensor s_2 determines its $s_2.I_{ELR}$ by computing $s_2.I_{ELR} = s_1.C_{ELR} \cap s_3.C_{ELR}$, where $s_1.C_{ELR}$ and $s_3.C_{ELR}$ are determined by $s_1.ELR_{org}$ and $s_3.ELR_{org}$, respectively. Similar to sensor s_2, the unreliable sensor s_6 will compute $s_6.I_{ELR} = s_9.C_{ELR}$, where $s_9.C_{ELR}$ is determined by $s_9.ELR_{org}$. The unreliable sensors s_{11} and s_7 compute $s_{11}.I_{ELR} = s_9.C_{ELR} \cap s_{10}.C_{ELR} \cap s_{12}.C_{ELR}$ and $s_7.I_{ELR} = s_5.C_{ELR} \cap s_9.C_{ELR}$, respectively. Since there exists no neighbor with smaller degree of unreliability than $C_u(s_{11})$ and $s_{11}.ELR_{org} \subseteq s_{11}.I_{ELR}$, sensor s_{11} sets $s_{11}.ELR_{dpc}$ by $s_{11}.I_{ELR}$. Then, it sends the information of $s_{11}.ELR_{dpc}$ to its unreliable neighbor s_7 which has larger degree of unreliability than itself. Upon receiving the information, sensor s_7 improves its I_{ELR} measurement by deriving $s_7.I_{ELR} = s_7.I_{ELR} \cap s_{11}.C_{ELR}$, where $s_{11}.C_{ELR}$ is determined by $s_{11}.ELR_{dpc}$. Then, sensors s_2, s_6, s_7, and s_{11} complete the *DPC* phase and initiate the *RC* phase.

In the *RC* phase, each sensor initially sets its I_{ELR} by ELR_{dpc}. Since there exists no neighbor that has larger degree of unreliability than $C_u(s_2)$ and the area size of $s_2.I_{ELR}$ is not smaller than that of $s_2.ELR_{dpc}$, sensor s_2 will set $s_2.ELR_{rc}$ by $s_2.ELR_{dpc}$. This means that $s_2.ELR_{rc}$ is determined according to the *ELR* measurements from its reliable neighbors s_1 and s_3. Similar to sensors s_2 and s_7, sensor s_6 will determine $s_6.ELR_{rc}$ and $s_7.ELR_{rc}$ based on the information of $s_6.ELR_{dpc}$ and $s_7.ELR_{dpc}$, respectively. Then, sensor s_7 will send the information $s_7.ELR_{rc}$ to its neighbor s_{11} since $C_u(s_7) > C_u(s_{11})$. Upon receiving the information $s_7.ELR_{rc}$, sensor s_{11} further improves its I_{ELR} measurement by calculating $s_{11}.I_{ELR} = s_{11}.I_{ELR} \cap s_7.C_{ELR}$, where $s_{11}.C_{ELR}$ is determined by $s_{11}.ELR_{rc}$ since $C_u(s_{11}) < C_u(s_7)$. Since the area size of $s_{11}.I_{ELR}$ is smaller than that of $s_{11}.ELR_{dpc}$, sensor s_{11} sets $s_{11}.ELR_{rc}$ to $s_{11}.I_{ELR}$. As a result, sensors s_2, s_6, s_7, and s_{11} complete the location correction and become reliable nodes again.

4.3. Analysis of localization improvement in error correction

In order to simplify the complexity of analysis, we analyze the localization improvement under the assumption that the sensors are uniformly deployed in this subsection. In the performance study, most of the experiments will be examined in the environment of randomly deployed sensor networks. Recall that the communication range of a sensor is r. Let the width and length of the monitoring region R be W and L, respectively. Herein, the unreliable sensor, which has the location error and leads to a location-aware routing error, is referred to as the *damage node*. The improvement of localization accuracy for the damage node by applying the proposed scheme in error correction will be analyzed in this subsection.

Assume that a sensor has location error and its localization accuracy is zero if its *ELR* size is $2r \times 2r$. An *ELR* with size $2r \times 2r$ means that the *ELR* has the maximal bounding box without being reduced by mobile anchor. Moreover, decreasing the area size of *ELR* will increase the localization accuracy of the sensor. The localization accuracy of sensor s_i, denoted by $A(s_i)$, can be measured by the following equation. Recall that the notation $|s_i.ELR|$ denotes the area size of $s_i.ELR$.

$$A(s_i) = \begin{cases} \dfrac{4r^2 - |s_i.ELR|}{4r^2} \times 100\%, & \text{if } s_i.ELR \text{ is defined} \\ 0\%, & \text{Otherwise.} \end{cases} \quad (4)$$

Notice that the value of $|s_i.ELR|$ in Eq. (4) will be set to $4r^2$ if the damage node s_i discards the localization information and resets itself to the "undefined" status before correction.

The W and L can be expressed by λr and $k\lambda r$, respectively. Let the average width and length of the *ELR*s of the sensors be w and l, where w and l can be expressed by ar and br, respectively. Thus, the area size of the monitoring region is $k(\lambda r)^2$. Assume that there are n sensors uniformly deployed in region R. The average number of the deployed sensors in each unit square, denoted by q, can be determined by

$$q = \frac{n}{k\lambda^2 r^2}. \quad (5)$$

Expression (5) is used for estimating the square area with size $\delta r \times \delta r$, which contains at least one deployed sensor. The value of δ can be determined as follows.

$$\delta r \times \delta r \times q = \frac{\delta^2 r^2 n}{k\lambda^2 r^2} = \frac{\delta^2 n}{k\lambda^2} = 1, \quad \delta = \frac{\lambda\sqrt{k}}{\sqrt{n}}.$$

Assume that a damage node, say sensor s_v, is created due to the unexpected events such as a storm or malicious removal. By applying the proposed *ALCP*, sensor s_v executes the process of the location error detection, reports the exception, and discards its location information. The *ELR* information of the farther neighbors of sensor s_v can be used to obtain a smaller $|s_v.ELR|$ and hence improve the localization accuracy of $A(s_v)$. Since all sensors are uniformly deployed in region R, the scale δr can evaluate the locations of the farther neighbors of sensor s_v. Let (x, y) be the new location of sensor s_v. As shown in Fig. 8, consider that sensors s_i and s_j are the farther neighbors of sensor s_v at the left-top and right-bottom corners, respectively. The locations of sensors s_i and s_j can be set to $(x - d, y - d)$ and $(x + d, y + d)$, where

$$d = \delta r \times \left\lfloor \frac{r}{\delta r} \right\rfloor = \frac{r\lambda\sqrt{k}}{\sqrt{n}} \times \left\lfloor \frac{\sqrt{n}}{\lambda\sqrt{k}} \right\rfloor. \quad (6)$$

Hence, the range of d can be derived from Eq. (6).

$$\frac{r\lambda\sqrt{k}}{\sqrt{n}} \times \left(\frac{\sqrt{n}}{\lambda\sqrt{k}} - 1 \right) < d \le \frac{r\lambda\sqrt{k}}{\sqrt{n}} \times \frac{\sqrt{n}}{\lambda\sqrt{k}}$$

$$r\left(1 - \frac{\lambda\sqrt{k}}{\sqrt{n}}\right) < d \le r, \quad 0 \le r - d < \frac{r\lambda\sqrt{k}}{\sqrt{n}}.$$

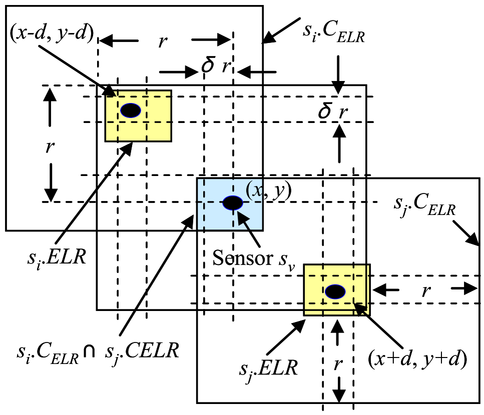

Fig. 8. The *ELR* estimation of the damage node s_v estimated by the density of deployed sensors, the average width, and length of the *ELR*s of the reliable sensors.

Fig. 8 shows how the damage node s_v estimates its *ELR*. In Fig. 8, the locations of sensors s_i and s_j can be represented by using the location (x, y) of sensor s_v. By applying the proposed *ALCP*, reliable sensors s_i and s_j provide $s_i.C_{ELR}$ and $s_j.C_{ELR}$ for the location error correction. As a result, the $s_v.ELR$ can be bounded in the area evaluated by the following expression.

$$\left(x+d-\frac{ar}{2}-r, y+d-\frac{br}{2}-r\right) - \left(x-d+\frac{ar}{2}+r, y-d+\frac{br}{2}+r\right).$$

Let w' and l' be the width and length of $s_v.ELR$, respectively. The value w' can be estimated in Eq. (7).

$$\begin{aligned} w' &\le \left(x-d+\frac{ar}{2}+r\right)-\left(x+d-\frac{ar}{2}-r\right) \\ &\le ar+2(r-d) < ar+2\frac{r\lambda\sqrt{k}}{\sqrt{n}}. \end{aligned} \tag{7}$$

Similar to the estimation of w', the value of l' can be estimated in Eq. (8).

$$l' \le br+2(r-d) < br+2\frac{r\lambda\sqrt{k}}{\sqrt{n}}. \tag{8}$$

Let u denote the average localization accuracy of reliable sensors before the occurrence of location error, where value u can be obtained by Eq. (9).

$$\begin{aligned} u &= \frac{4r^2 - w\times l}{4r^2}\times 100\% \\ &= \frac{4r^2-abr^2}{4r^2}\times 100\% = \left(1-\frac{ab}{4}\right)\times 100\%. \end{aligned} \tag{9}$$

Herein, a higher value of u indicates that the sensor network is constructed by the sensors with higher average localization accuracy.

Recall that the localization accuracy of s_v in Eq. (4) will be set to 0%, or the value $|s_v.ELR|$ will be set to $4r^2$ when the damage node s_v discards the localization information. That is, the accuracy $A(s_i)$ of a sensor achieves 0% if the real location of the sensor is out of its *ELR* due to the occurrence of accident. On the contrary, that the value of $A(s_i)$ is 100% means that the sensor s_i has the location information of the point where it is located. The localization correction by applying *ALCP* can improve the localization accuracy of s_v from 0% to $A(s_v)$, where value $A(s_v)$ can be measured by the following Eqs. (10)–(15). The high value of $A(s_v)$ implies the localization accuracy of s_v, which can be significantly improved in the localization correction.

$$A(s_v) = \frac{4r^2-|s_v.ELR|}{4r^2}\times 100\% \tag{10}$$

$$= \left(1-\frac{w'\times l'}{4r^2}\right)\times 100\% \tag{11}$$

$$\ge \left(1-\frac{\left(a+2\frac{\lambda\sqrt{k}}{\sqrt{n}}\right)r\times\left(b+2\frac{\lambda\sqrt{k}}{\sqrt{n}}\right)r}{4r^2}\right)\times 100\% \tag{12}$$

$$= \left(1-\frac{ab}{4}\right)\times 100\% - \left(\frac{\lambda\sqrt{k}}{2\sqrt{n}}(a+b)+\frac{\lambda^2 k}{n}\right)\times 100\% \tag{13}$$

$$= u - \left(\frac{\lambda(a+b)\sqrt{k}}{2\sqrt{n}}+\frac{\lambda^2 k}{n}\right)\times 100\% \tag{14}$$

$$= u - \Delta, \quad \text{where } \Delta = \left(\frac{\lambda(a+b)\sqrt{k}}{2\sqrt{n}}+\frac{\lambda^2 k}{n}\right)\times 100\%. \tag{15}$$

In Eq. (10), the new estimated *ELR* of sensor s_v and its area size are represented by $s_v.ELR$ and $|s_v.ELR|$, respectively. Notice that the value of $A(s_v)$ will be in the range of 0%–100% because $0 \le |s_v.ELR| \le 4r^2$. Since the width and length of $s_v.ELR$ are measured by w' and l', Eq. (11) can be derived from Eq. (10). Substituting Eqs. (7) and (8) into (11), Eq. (12) can be obtained. Eq. (14) can be further derived by substituting Eq. (9) into Eq. (13).

Herein, we summarize two observations from Eqs. (14) and (15). The sensors with smaller *ELR*s also indicate that they have better average accuracy. The observation can be verified by Eq. (15). In Eq. (15), the improvement of the localization accuracy by applying the proposed *ALCP* can be determined by the parameters u and Δ. As shown in Eq. (15), the small values of a and b and the large value of u lead to a high accuracy $A(s_v)$. The first observation can be verified. The second observation is that the accuracy $A(s_v)$ is increased with the corrections of location error by applying the proposed *ALCP*. The area size of $|s_v.ELR|$ depicted in Eq. (10) can be decreased by correcting the location errors in *ALCP*. This result can be verified by examining that decreasing the value of $|s_v.ELR|$ will increase the value of $A(s_v)$.

Moreover, Eq. (14) shows that the improvement of $A(s_v)$ by applying *ALCP* increases with the number of sensors, given sensors with fixed initial localization accuracy. Although the number of sensors can impact the improvement of the localization accuracy, it is still important to derive the minimal number of the sensors that is required to guarantee that *ALCP* can improve the location accuracy, i.e., $A(s_v) > 0\%$. We assume that $A(s_v) > 0\%$ aims to derive the relationship between n and $A(s_v)$ after considering the values of a, b, k, and λ to be constant. Eq. (15) shows that the summation of value u and decay value Δ should be greater than zero. Therefore, the minimal number of sensors can be derived as Eq. (17).

Assume $A(s_v) > 0\%$

$$\Leftrightarrow \left(1-\frac{ab}{4}\right) - \left(\frac{\lambda\sqrt{k}}{2\sqrt{n}}(a+b)+\frac{\lambda^2 k}{n}\right) > 0 \tag{16}$$

$$\Leftrightarrow ((4-ab)-\lambda^2 k)^2 - (2\lambda\sqrt{kn}(a+b))^2 > 0$$

$$\Leftrightarrow (4-ab)^2 n^2 - 4\lambda^2 k(a^2+b^2+8)n + 16\lambda^4 k^2 > 0$$

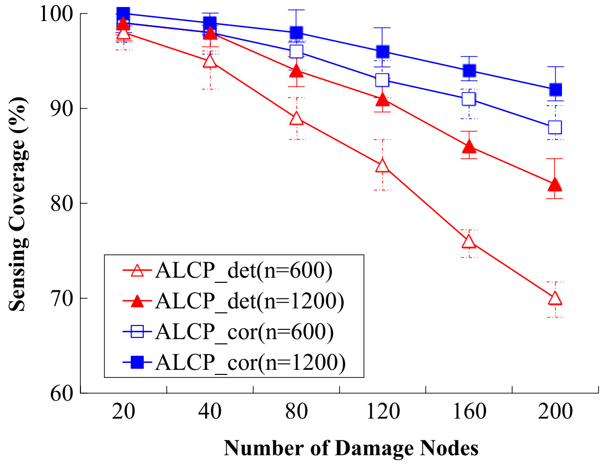

Fig. 9. The impact of the number of damage nodes on the sensing coverage ($u = 95\%$).

$$\Leftrightarrow n > \frac{2\lambda^2 k(\zeta + \sqrt{\zeta^2 + 4(4-ab)^2})}{(4-ab)^2},$$

$$\text{where } \zeta = a^2 + b^2 + 8. \tag{17}$$

When the number of sensors deployed in the monitoring region is more than the minimal number of sensors, depicted in Eq. (17), the localization accuracy $A(s_v)$ can be improved by applying the proposed *ALCP*. For example, if the values W, L, u, and r are set to 500, 500, 95%, and 50%, respectively, the number of sensors deployed in WSN should be greater than 413 when $A(s_v) > 0\%$ is required for the location correction.

5. Performance study

This section examines the performance of the proposed *ALCP* against the existing bounding box techniques in terms of the localization accuracy, the number of routing fault nodes, the number of routing errors, and the routing length by using the Glomosim simulator [9]. The experimental environment is described below. The static sensors (400–1200 sensors) are randomly deployed in a 500 m × 500 m monitoring region. The communication and sensing range of each sensor are set at 50 m. Each performance result was obtained from the average results of 100 experiments. The 90% confidence interval is always less than 10% of the reported values. Initially, each deployed sensor is localized by an *ELR*. The number of accidents that happen within a given period depends on the accident types. The impact of location errors caused by the accidents also depends on the application of wireless sensor networks. For example, the deserts in the Junggar Basin have strong breeze with strength of 17 m/s for an average of 80 days in a year [11]. In the experiment, the damaged node (location error node) will be randomly produced from 30 to 100 days. The damage nodes are randomly selected from the deployed sensors and the moved distance is set from 10 to 200 m. In the simulation, the proposed *ALCP* algorithm is triggered every day to measure its improvements. Each sensor maintains its *ELR* location information and exchanges its information of *ELR* and ID with its neighbors when it detects the variation of its neighbors. The design of *ALCP* consists of location error detection and correction. To observe their individual contributions, the schemes *ALCP_det* and *ALCP_cor* are used to examine the impact of location errors on the sensors with the detection function and with the detection and correction functions, respectively. In this paper, the abbreviations *Bounding*, *ALCP_det*, and *ALCP_cor* are used to represent the experimental results. The location-aware routing GPSR [12] is applied in the experiments to evaluate the improvement on routing performances. When the GPSR is applied in the experiments, the location of each sensor s_i is estimated by the center location of its own *ELR* at time t, denoted by $s_i.ELR_t$.

Fig. 9 examines the impact of the location errors on the sensing coverage by varying the number of damage nodes. The sensing coverage of the sensors is measured by the real location of the sensors in the experiment. The monitoring area is partitioned into several equal-sized grids. The sensing coverage is measured by calculating the percentages of the grids covered by the sensing area of the sensors to the total grids. The grids that are only covered by the damage nodes will be considered as coverage loss since the damage nodes cannot report the correct location for the monitoring events. In general, the number and size of coverage holes in the WSN increase with the number of damage nodes. Since the *ALCP_cor* can correct the *ELR* information of the damage nodes, it achieves better sensing coverage than *ALCP_det*.

The damage nodes will reduce the localization accuracy of WSN. Fig. 10(a) and (b) investigate the localization accuracy of WSN by applying three compared schemes under various initial localization accuracies of the sensors. The localization accuracy of WSN N, denoted by $A(N)$, is measured in Eq. (1), where $s_i \in N$ and $A(s_i)$ is defined in Eq. (4).

Fig. 10(a) and (b) investigate the localization accuracy with the initial localization accuracy of 95% and 99.5%, respectively. A comparison of the two figures shows that both *ALCP_det* and *ALCP_cor* schemes have better performance in terms of localization accuracy if the sensors initially have higher localization accuracy.

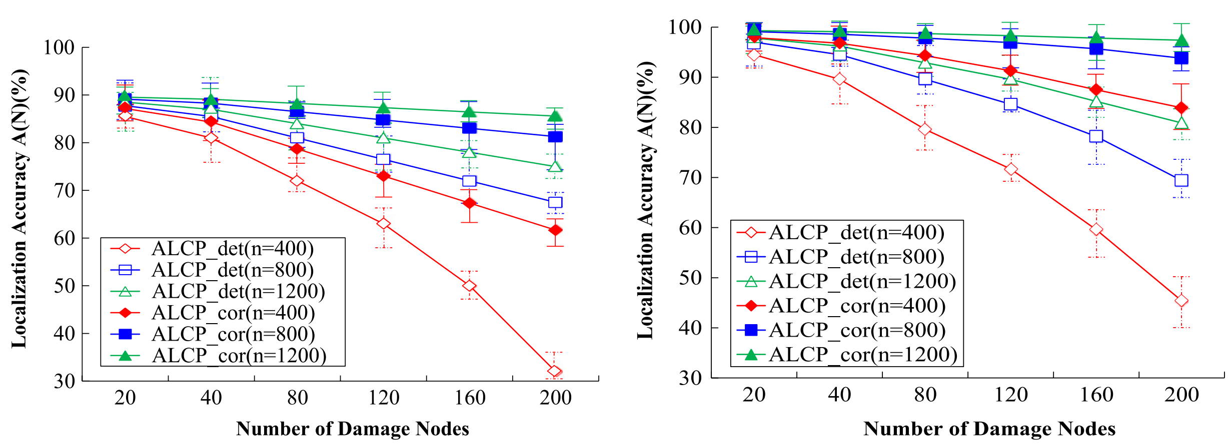

(a) Initial localization accuracy of the sensors is with 95%.

(b) Initial localization accuracy of the sensors is with 99.5%.

Fig. 10. ALCP is always applied but with and without correction under various initial localization accuracies of the sensors.

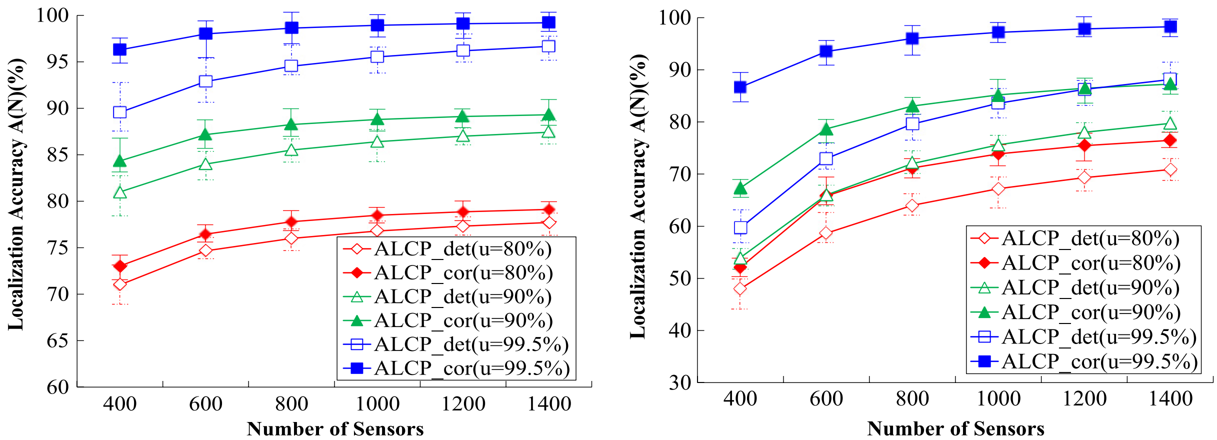

(a) The number of damage nodes is set to 40.

(b) The number of damage nodes is set to 160.

Fig. 11. The localization accuracy of WSN with and without applying the proposed *ALCP* by varying the initial localization accuracies of the sensors and network densities.

The reason is that the sensors with higher initial localization accuracies can help the damage nodes to correct their locations with more accuracy. There are general observations from the experimental results of Fig. 10(a) and (b). First, the localization accuracy of WSN generally decreases with the number of damage nodes. Another observation is that both the proposed *ALCP_det* and *ALCP_cor* increase the localization accuracy with the network density of WSN. The reason is that the localization accuracy of a damage node will be improved when the number of its neighboring *ELR*s is increased. Since the *ALCP_cor* can correct the *ELR* information of the damage nodes, it obtains better location accuracy than the other compared approaches when low ratio of the number of damage nodes to the number of sensors is considered.

Let location error ratio refer to the ratio of the number of damage nodes to the number of all sensor nodes. In Fig. 10(a), let us fix the number of damage node by a constant value of 160. Although *ALCP_det* did not correct any location error, the average localization accuracies of *ALCP_det* increase with the number of sensor nodes. This fact can be easily observed from Fig. 10(a) since *ALCP_det* with $n = 1200$ has better performance than *ALCP_det* with $n = 400$ and $n = 800$. This occurs because the number of damage nodes is fixed at 160 but the number of sensor nodes is increased. Therefore, the location error ratio is decreased when the number of sensors increases, which raises the average localization accuracy of the given wireless sensor network. It is interesting to compare the curves of *ALCP_det* with $n = 800$ and *ALCP_cor* with $n = 400$. The *ALCP_det* with $n = 800$ has better performance than *ALCP_cor* with $n = 400$. This occurs because *ALCP_det* with $n = 800$ has low location error ratio which improves the average localization accuracy, especially when the location error ratio is low. As a result, the average localization accuracy of *ALCP_cor* with $n = 400$ becomes lower than that of *ALCP_det* with $n = 800$ in all cases.

Given different initial localization accuracies, Fig. 11 measures the average localization accuracies of *ALCP_det* and *ALCP_cor* by varying the number of sensor nodes ranging from 400 to 1400. The performances of *ALCP_det* and *ALCP_cor* are examined with the initial localization accuracy of 80%, 90%, and 99.5%. In the experiments, the numbers of damage nodes are set to 40 and 80 in Fig. 11(a) and (b), respectively. In general, as shown in Fig. 11(a), the average localization accuracies of all curves increase with the number of sensor nodes. Let the location error ratio refer to the ratio of the number of damage nodes to the number of all sensor nodes. Although *ALCP_det* did not correct any location error, the average localization accuracies of *ALCP_det* with $u = 80\%$, 90% and 99.5% increased with the number of sensor nodes. This occurs because the number of damage nodes is fixed to 40 but the number of sensor nodes is increased. Therefore, the location error ratio is decreased when the number of sensors increases, which raises the average localization accuracy of the given wireless sensor network. As shown in Fig. 11(a), the *ALCP_cor* always outperforms *ALCP_det* when the initial localization accuracies (the value of u) of the two compared mechanisms are set with the same value. This occurs because *ALCP_det* only detects the location errors of damage nodes without correcting any location error while *ALCP_cor* not only detects but also corrects the location errors of the damage nodes. This also indicates that the *ALCP_cor* reduces the number of damage nodes and hence improves the average localization accuracy in all cases, as compared with the *ALCP_det* under the same value of u. In Fig. 11(b), the number of damage nodes is set to 80 which is larger than that set in Fig. 11(a). In general, the curves of Fig. 11(b) are similar to those of Fig. 11(a). It is interesting to compare the curves of *ALCP_det* with $u = 99.5\%$ and *ALCP_cor* with $u = 90\%$. The results of the two curves increase with the number of sensor nodes. However, the curve of *ALCP_det* with $u = 99.5\%$ increases more significantly than that of *ALCP_cor* with $u = 90\%$. This occurs because *ALCP_det* with $u = 99.5\%$ has high initial localization accuracy which improves the average localization, especially when the location error ratio is low. As a result, the average localization accuracy of *ALCP_cor* with $u = 90\%$ becomes lower than that of *ALCP_det* with $u = 99.5\%$ when the number of sensor nodes is larger than 1200. This means that *ALCP_cor* has better performance of location correction than *ALCP_det* in terms of the localization accuracy when the location error ratio is high.

Fig. 12(a) and (b) examine the performance of *ALCP_det* and *ALCP_cor* in the network scenario where all sensors are uniformly deployed. In the experiments, the network density, initial localization accuracy, and the number of damage nodes are fixed. The performance depicted in Fig. 11(a) and (b) is similar to those examined in the uniform deployment, as shown in Fig. 12(a) and (b). Comparing Fig. 12(a) with Fig. 11(a), the localization accuracies of *ALCP_det* and *ALCP_cor* in the uniform deployment scenario outperform those in the random deployment scenario. When the number of damage nodes increases, the performance of *ALCP_cor*($u = 80\%$) and *ALCP_cor*($u = 90\%$) in the uniform deployment, as depicted in Fig. 12(b), will be better than those of *ALCP_det*($u = 90\%$) and *ALCP_det*($u = 99.5\%$), as shown in Fig. 11(b), respectively. This is because the damage nodes in the uniform deployment are able to communicate with more neighbors than those in random deployment when they move to the new locations in accidents. The results reveal that the damage nodes in the uniform deployment, as depicted in Fig. 12(b), will obtain more average chances from neighbors to execute

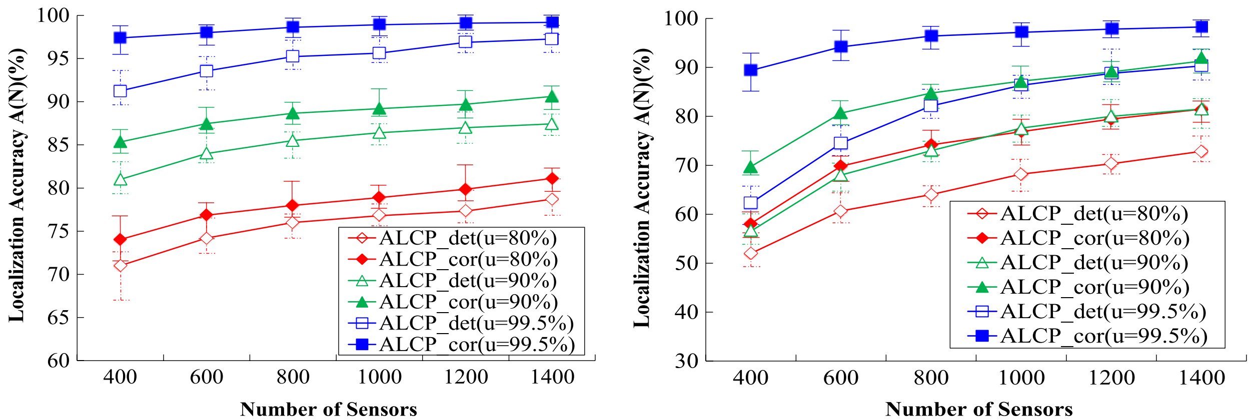

(a) The number of damage nodes is set to 40. (b) The number of damage nodes is set to 160.

Fig. 12. The localization accuracy of WSN with and without applying the proposed *ALCP* by varying the initial localization accuracies of the sensors and network densities when the sensors are deployed uniformly.

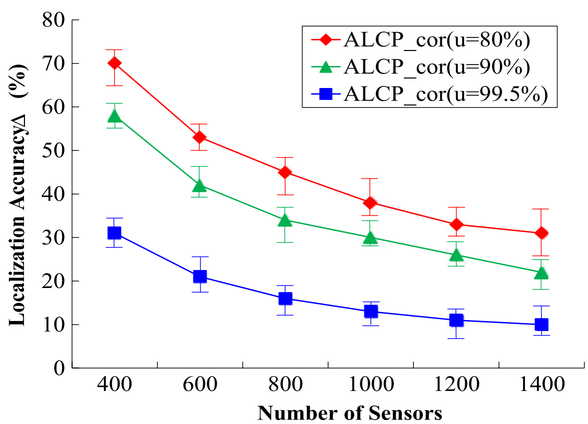

Fig. 13. The decay value of the initial localization accuracy examined for *ALCP_cor* by varying the network densities.

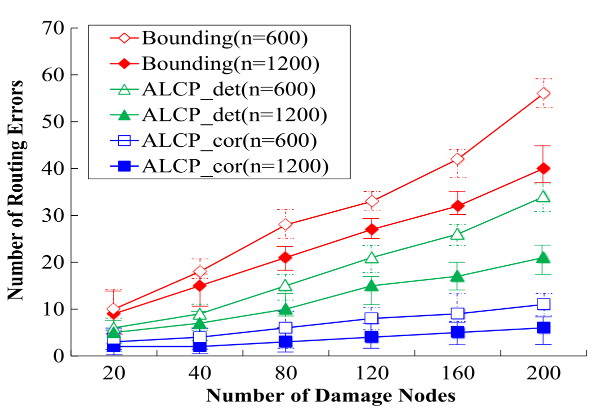

Fig. 14. The impact of the number of damage nodes on the number of routing errors.

the location error detection and correction than the random deployment, as shown in Fig. 11(b).

A WSN with low decay value indicates its localization accuracy will decrease slowly. It also reveals that the applications on the WSN will have low impact of the localization accuracy on the location errors. The decay values investigated in Fig. 13 are useful to observe the following properties. (1) If the initial localization accuracy is fixed, how many numbers of the deployed sensors are needed to obtain a low decay value. (2) If the number of the deployed sensors is fixed, how much initial localization accuracy is needed to obtain a low decay value. The decay value is important

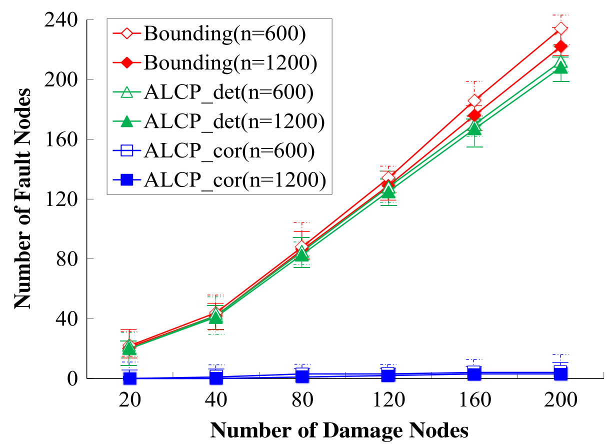

Fig. 15. *ALCP_cor* creates few routing fault nodes than *Bounding* and *ALCP_det* by executing GPSR routing protocol.

to construct the WSN with robustness to the location errors. Fig. 13 investigates the decay value Δ of initial localization accuracy depicted in Eq. (14) by varying the network densities. As shown in Fig. 13, *ALCP_cor* with high initial localization accuracy leads to low decay value and hence achieves better localization accuracy. The decay value decreases with the number of sensors since a large number of sensors provide more opportunities to correct the location of damage node. Moreover, with fixed number of sensors, the sensors with high initial localization accuracy have smaller decay value than the sensors with low initial localization accuracy. The reason is that the sensors with high initial localization accuracy provide more accurate *ELR* information to correct the location of damage node.

Figs. 14–17 show the experimental results of the compared *ALCP_cor*, *ALCP_det*, and *Bounding* approaches in terms of number of routing errors, the number of routing fault nodes, and the length of routing path. The *Bounding* scheme [20,6] is a well-known localization mechanism which provides each sensor with location information presented by a bounding box. However, the *Bounding* scheme does not consider the functions of location error detection or correction. In *Figs.* 14–17 *and* 21, the *Bounding* scheme is used in experiments to examine the impact of location errors to the WSN without applying ALCP. The initial localization accuracy of the sensors is set at 99.5%. As shown in Fig. 14, the number of routing errors of the compared schemes generally increases with the number of damage nodes. The *ALCP_cor* produces fewer routing errors than *Bounding* and *ALCP_det* approaches since it corrects the *ELR* information of damage nodes. In the *Bounding*

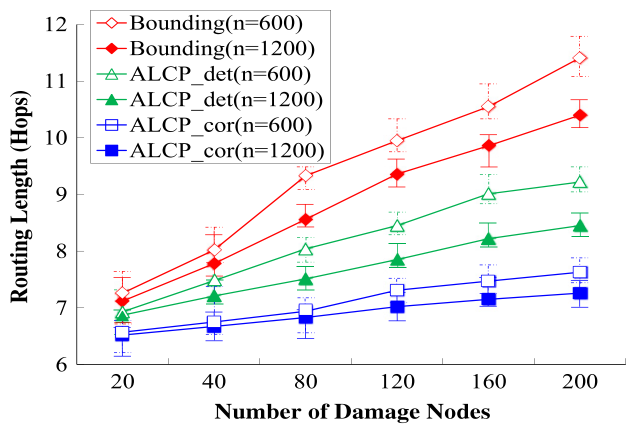

Fig. 16. The impact of the number of damage nodes on the routing length by applying *Bounding*, *ALCP_det*, and *ALCP_cor* schemes.

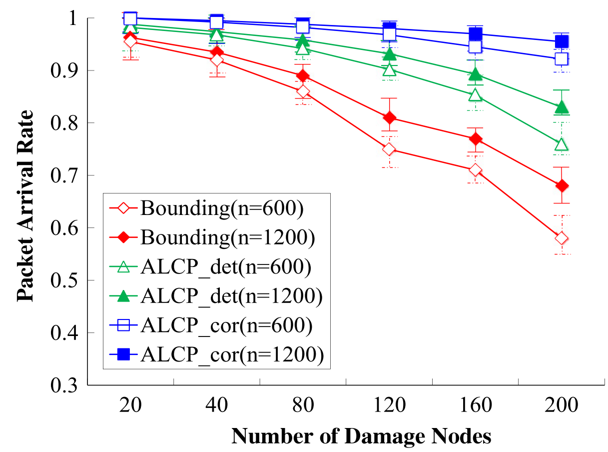

Fig. 17. Comparison of routing performance among *Bounding*, *ALCP_det*, and *ALCP_cor* on GPSR routing protocol in terms of the packet arrival rate.

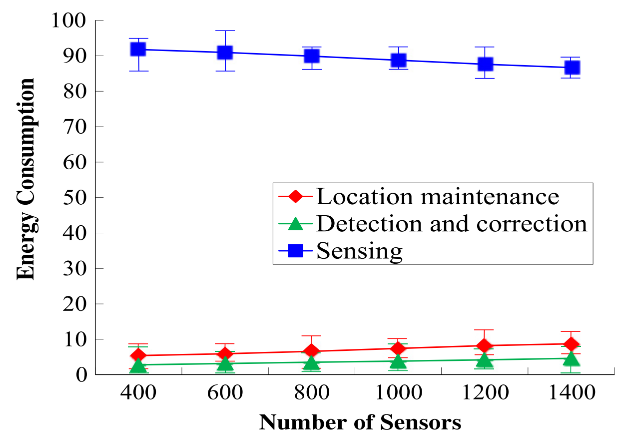

Fig. 18. The cost and overhead examined for *ALCP_cor* by varying the network densities. The initial localization accuracy and the number of damage nodes are set by $u = 95\%$ and 160, respectively. (For interpretation of the references to color in this figure legend, the reader is referred to the web version of this article.)

scheme, the damage nodes always apply the initial *ELR* information for routing and hence the GPSR cannot work well based on the inaccurate location information. As a result, the *Bounding* scheme significantly increases the number of routing errors when the number of damage nodes is increased. Moreover, the *ALCP_det* can detect the damage nodes and prohibit them from routing the packet in WSN. Thus, *ALCP_det* has better performance than *Bounding* approach in terms of the number of routing errors.

Since the damage nodes will discard the *ELR* information and reset itself to the "undefined" status, the nodes will be not used to route the packets in WSN. These nodes are referred to as *routing fault nodes* which cannot participate in the routing packet in the routing task. In Fig. 15, the proposed *ALCP_cor* can correct the *ELR* information of the damage nodes such that most of the sensors can participate in the location-aware routing. Without correcting the location of damage nodes, the *Bounding* scheme creates a lot of routing errors when applying the GPSR routing protocol.

Fig. 16 further investigates the routing length by applying the compared localization approaches. The location-aware GPSR is used as the routing protocol to construct the routing path. The *Bounding* approach is not developed with the location error detection and hence it increases both numbers of routing faults and the routing hops. Since the damage nodes can be identified in *ALCP_det*, the *ALCP_det* reduces both numbers of the routing faults and routing hops. Further, the *ALCP_cor* has more routing opportunities than that of *ALCP_det* and hence results in shorter routing length than that of *ALCP_det*. As shown in Fig. 16, the proposed *ALCP_cor* has higher performance in terms of the routing length than the other two schemes.

Fig. 17 investigates the routing performance of *Bounding*, *ALCP_det*, and *ALCP_cor* in terms of the packet arrival rate. In Fig. 15, the proposed *ALCP_cor* creates few routing fault nodes when location errors occur in WSN. Increasing the opportunity of packet routing will also enhance the routing performance in terms of the packet arrival rate. As shown in Fig. 17, *ALCP_cor* significantly achieves higher packet arrival rate than the other schemes because it detects and corrects the location errors and hence improves the location accuracies of sensors.

Fig. 18 investigates the overheads of ALCP by varying the network densities. In general, two costs will be produced when the ALCP is applied. First, a constant cost, also referred to the *location maintenance cost*, is produced due to the maintenance of neighboring location information. This cost is increased with the number of location information exchanged among neighboring nodes within a given time. Another cost, referred to as the *detection and correction cost*, is produced when executing location error detection and correction. Each location-aware application has its own requirement of location accuracy. Therefore, the two costs highly depend on the location accuracy required by the applications. Fig. 18 reveals that the overheads of ALCP increase with the number of deployed sensors. This occurs because the number of neighbors increases with the number of sensors. Hence, the location maintenance cost will be increased when the number of sensors is increased. In general, the overheads, including *location maintenance cost* and *detection and correction cost*, increase from 8% to 14% when the number of sensors varies from 400 to 1400 sensors. As shown in Fig. 18, the energy consumption of sensing task (the curve with the blue color) is much higher than those of location maintenance task and location detection and correction task. Therefore, the proposed ALCP is energy efficient while improving the location accuracy. This also indicates that ALCP is cost effective.

Let $R_{\max}$ and r_{stable} be the maximum communication range and the stable radio range of each sensor, respectively. With the consideration of irregularity of communication ranges [2,27], we assume that the communication range r of each sensor varies in the range $0.8R_{\max} \leqq r \leqq R_{\max}$. As shown in Fig. 19, the shadow region depicts the actual transmission range of sensor s_i. Taking the radio irregularity into consideration, two sensors with distance d_r, where $0.8R_{\max} \leqq d_r \leqq R_{\max}$, may or may not be able to communicate with each other directly. In order to observe the impact of ALCP on irregular radio communication, the neighboring information received from beacons within a given time will be collected together for calculating $C_u()$. If sensor x receives any

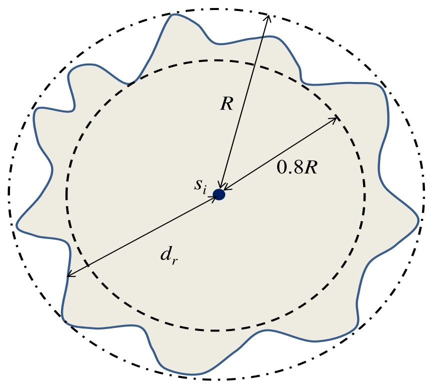

Fig. 19. The transmission range of sensor s_i varies ranging from 0.8R to R.

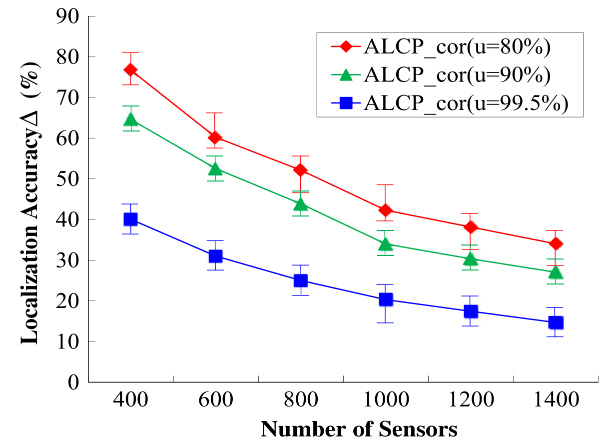

Fig. 20. The decay value of the initial localization accuracy examined for *ALCP_cor* by varying the network densities in irregular radio communication.

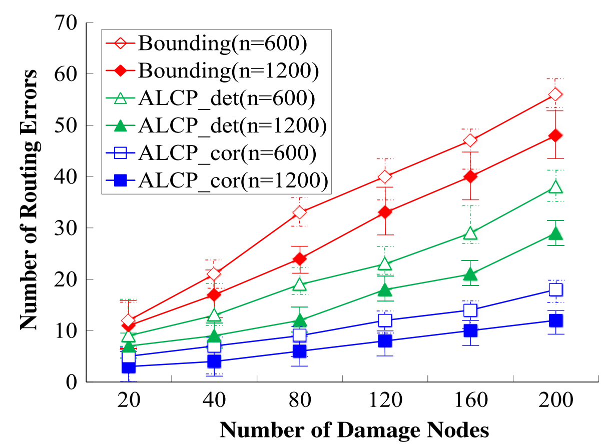

Fig. 21. The impact of the number of damage nodes on the number of routing errors when the irregular radio range is applied.

beacon from sensor y in a given time, sensors x and y will be considered as neighbors when $C_u()$ is calculated.

In ALCP, each sensor informs its existence to the neighboring nodes by the beacons and receives the messages from their neighbors. In the duration time, each sensor calculates its value of $C_u()$ by the received messages. When the duration time ends, the sensors exchange the value of $C_u()$ with their neighbors then initiate the location error detection in the *DPC* phase. If the location errors occur, the *RC* phase will be executed to further correct the location information. Since the location errors do not occur frequently, the frequency of the beacons might be set to a few seconds while a number of minutes can be set for the duration time. In order to observe the impact of ALCP on irregular radio communication, the neighboring information received by beacons in each duration time will be collected together for calculating $C_u()$. If sensor x has the message received in the duration time from sensor y, sensors x and y are neighbors when $C_u()$ calculating.

Fig. 20 examines the performance of ALCP in terms of the decay value of the localization accuracy by considering the irregularity of communication range. The curves in Fig. 20 are similar to those in Fig. 13, which applies the regular radio model. In comparison, all curves drop about 7% when the irregular radio range is applied. The major reason is that the reliable communication zone in an irregular radio range is smaller than that in a regular radio range. This indicates that the average number of the neighboring nodes is reduced, and hence the size of the intersected area of the neighboring nodes' *ELRs* is increased. As a result, the area size of I_{ELR} is increased, reducing the localization accuracy. To reduce the impact of irregular radio range, the proposed ALCP collects neighboring information periodically. The neighbor relation can be identified according to several collections of neighboring information, and hence ALCP reduces the impact of irregular radio range. Therefore, compared with the regular radio model, the performance drop of ALCP, by applying the irregular radio model, is not significant in terms of localization accuracy. Fig. 21 additionally investigates the impact of irregular radio range on the routing errors. As shown in Fig. 21, the number of routing errors by applying the irregular radio communication will be increased with the number of damage nodes. In comparison, the number of routing errors in Fig. 21 is greater than that in Fig. 14, which applies regular radio range. The increasing ratio is about 6%.

6. Conclusions

In wireless sensor networks, location information is very important for most applications. In recent years, a number of bounding box localization approaches have been proposed to save the hardware cost and energy consumption of sensor nodes. However, sensor nodes could be moved accidentally, raising location error problems in an outdoor environment. Based on the neighboring sensors' *ELR* information, this paper proposed the *ALCP* location detection and correction approaches which aim at detecting and subsequently correcting the location error. Hence the localization accuracy of the sensor nodes can be significantly improved. Based on the location information created by the bounding box approach, the proposed *ALCP* approach observes the properties of neighboring *ELR* information and applies these properties to detect and correct the location errors of sensor nodes. In performance study, we further investigate the contributions of *ALCP_det* and *ALCP_cor* schemes. The schemes *ALCP_det* and *ALCP_cor* are used to examine the impact of location errors on the sensors with the detection function and with the detection and correction functions, respectively. Performance results show that the *ALCP_cor* scheme outperforms the *ALCP_det* scheme regarding the sensing coverage, localization accuracy, the number of routing errors, the routing length, and so on. The major reason is that the *ALCP_cor* scheme further applies the location correction function. Experimental results show that the proposed *ALCP* mechanism can improve the location accuracy of the sensor node which has been moved by accident and thus enhance the route performance when the GPSR routing protocol is applied.

References

[1] R. Anthony, M. Ghassemian, Automatic mobility status estimation in wireless self-organized networks, J. Comput. System Sci. 77 (2011) 305–321.

[2] L. Barrière, P. Fraigniaud, L. Narayanan, J. Opatrny, Robust position-based routing in wireless ad hoc networks with irregular transmission ranges, Wireless Commun. Mob. Comput. 3 (2003) 141–153.
[3] S. Capkun, K. Rasmussen, M. Cagalj, M. Srivastava, Secure location verification with hidden and mobile base stations, IEEE Trans. Mob. Comput. 7 (5) (2008) 470–483.
[4] X. Chen, A. Edelstein, Y. Li, M. Coates, M. Rabbat, A. Men, Sequential Monte Carlo for simultaneous passive device-free tracking and sensor localization using received signal strength measurements, in: IEEE/ACM IPSN, 2011, pp. 343–351.
[5] X. Chen, N.C. Rowe, J. Wu, K. Xiong, Improving the localization accuracy of targets by using their spatial–temporal relationships in wireless sensor networks, J. Parallel Distrib. Comput. 72 (2012) 1008–1018.
[6] V.H. Dang, V.D. Le, Y.K. Lee, S. Lee, Distributed push-pull estimation for node localization in wireless sensor networks, J. Parallel Distrib. Comput. 71 (2011) 471–484.
[7] W. Du, L. Fang, P. Ning, LAD: localization anomaly detection for wireless sensor networks, J. Parallel Distrib. Comput. 66 (2006) 874–886.
[8] A. Galstyan, B. Krishnamachari, K. Lerman, Distributed online localization in sensor networks using a moving target, in: IEEE IPSN, 2004.
[9] GloMoSim: global mobile information systems simulation library. http://pcl.cs.ucla.edu/projects/glomosim/.
[10] T. He, C. Huang, B. Lum, J. Stankovic, T. Adelzaher, Range-free localization schemes for large scale sensor networks, in: ACM MobiCom, 2003.
[11] http://www.lantianyu.net/pdf5%5Cts090012.htm.
[12] B. Karp, H.T. Kung, GPSR: greedy perimeter stateless routing for wireless networks, in: ACM MobiCom, 2000.
[13] M. Keally, G. Zhou, G. Xing, Sidewinder: a predictive data forwarding protocol for mobile wireless sensor networks, in: IEEE SECON, 2009.
[14] S. Kumar, T.H. Lai, A. Arora, Barrier coverage with wireless sensors, in: ACM MobiCom, 2005.
[15] S.P. Kuo, H.J. Kuo, Y.C. Tseng, The beacon movement detection problem in wireless sensor networks for localization applications, IEEE Trans. Mob. Comput. 8 (10) (2009) 1326–1338.
[16] S. Lee, E. Kim, C. Kim, K. Kim, Localization with a mobile beacon based on geometric constraints in wireless sensor networks, IEEE Trans. Wireless Commun. 8 (2009) 5801–5804.
[17] C. Liu, K. Wu, T. He, Sensor localization with ring overlapping based on comparison of received signal strength indicator, in: IEEE MASS, 2004.
[18] F. Mourad, H. Snoussi, F. Abdallah, C. Richard, A robust localization algorithm for mobile sensors using belief functions, IEEE Trans. Veh. Technol. 60 (2011) 1799–1811.
[19] J.P. Sheu, P.C. Chen, C.S. Hsu, A distributed localization scheme for wireless sensor networks with improved grid-scan and vector-based refinement, IEEE Trans. Mob. Comput. 7 (9) (2008) 1110–1123.
[20] J.P. Sheu, W.K. Hu, J.C. Lin, Distributed localization scheme for mobile sensor networks, IEEE Trans. Mob. Comput. 9 (4) (2010) 516–526.
[21] T.V. Srinath, Localization in resource constrained sensor networks using a mobile beacon with in-ranging, in: IEEE WOCN, 2006.
[22] V. Vivekanandan, V. Wong, Concentric anchor-beacons (CAB) localization for wireless sensor networks, in: IEEE ICC, 2006.
[23] V. Vivekanandan, V.W.S. Wong, Concentric anchor beacon localization algorithm for wireless sensor networks, IEEE Trans. Veh. Technol. 56 (5) (2007) 2733–2744.
[24] Y. Wei, Z. Yu, Y. Guan, Location verification algorithms for wireless sensor networks, in: IEEE ICDCS, 2007.
[25] G. Yang, D. Qiao, Barrier information coverage with wireless sensors, in: Proceedings of IEEE INFOCOM, 2009, pp. 918–926.
[26] S. Zhang, J. Cao, L. Chen, D. Chen, Accurate and energy-efficient range-free localization for mobile sensor networks, IEEE Trans. Mob. Comput. 9 (6) (2010) 897–910.
[27] G. Zhou, T. He, S. Krishnamurthy, J.A. Stankovic, Impact of radio irregularity on wireless sensor networks, in: ACM MobiSys, 2004.

Chao-Tsun Chang received the Ph.D. degree in Computer Science and Information Engineering from National Central University, Taiwan, in 2006. He is with the Department of Information Management, Hsiuping University of Science & Technology, Taiwan, as an Associate Professor in 2012. In the recent ten years, he has directed eleven researching projects including ten national NSC projects and seven information system developments. He published sixteen SCI indexed journal papers, including *IEEE TVT, IEEE Sensors, Computer Networks, ACM/Baltzer Journal of Wireless Networks*, and *Journal of Parallel and Distributed Computing*. Dr. Chang is a member of the IEEE Computer Society and Communication Society. His current research interests include Ad Hoc wireless networks, wireless sensor networks, cooperative radio networks, and mobile computing.

Chih-Yung Chang received the Ph.D. degree in Computer Science and Information Engineering from National Central University, Taiwan, in 1995. He is currently a Full Professor with the Department of CSIE at Tamkang University, Taiwan. Dr. Chang served as an Associate Guest Editor for many SCI indexed Journals, including *International Journal of Ad Hoc and Ubiquitous Computing* (IJAHUC 2011–2014), *International Journal of Distributed Sensor Networks* (IJDSN, 2012–2014), *IET Communications* (2011), *Telecommunication Systems* (TS, 2010), *Journal of Information Science and Engineering* (JISE, 2008) and *Journal of Internet Technology* (JIT, 2004 & 2008). He was an Area Chair of *IEEE AINA*'2005, *TANET*'2000, *TANET*'2010, *IEEE WisCom*'2005, *EUC*'2005 *IEEE ITRE*'2005, and *IEEE AINA* 2008, Program Co-Chair of *IEEE MNSA*'2005, *UbiLearn*'2006, *WASN*'2007, *ACM SAMnet*'2008, *IEEE AHUC*'2008, *iCube*'2010, *iCube*'2011, Workshop Co-Chair of *MSEAT*'2003, *MSEAT*'2004, *IEEE INA*'2005, *ICS*'2008, *NCS*'2009, *IEEE VCNA*'2009 and Publication Chair of *MSEAT*'2005 and *SCORM*'2006. Dr. Chang is a member of the IEEE Computer Society and Communication Society. His current research interests include Internet of Things, wireless sensor networks, Ad Hoc wireless networks, and LTE broadband technologies.

Tzu-Lin Wang received the B.S. and M.S. degrees in computer science and information engineering in 2007 and 2009, respectively, from Aletheia University, Taiwan. She is currently working toward the Ph.D. degree in the Department of Computer Science and Information Engineering at Tamkang University, Taiwan. Ms. Wang won numerous scholarships in Taiwan and has participated in many wireless sensor networking projects. Ms. Wang current research interests include wireless sensor networks, Ad Hoc wireless networks, mobile/wireless computing and WiMAX.